Supplement of Earth Syst. Sci. Data, 17, 4901–4932, 2025
https://doi.org/10.5194/essd-17-4901-2025-supplement


Open Access Earth System Science Data

*Supplement of*

# Observational ozone datasets over the global oceans and polar regions (version 2024)

**Yugo Kanaya et al.**

*Correspondence to:* Yugo Kanaya (yugo@jamstec.go.jp)

10

**Table S1.** Methods and uncertainties of CO, NOx, and CN observations associated with $O_3$ observations from ship cruises. See Table S7 for a list of acronyms.

| Label | Cruise | CO, NOx, CN instrumentation | Uncertainty |
|---|---|---|---|
| S1 | MR12: MR12-02 | Thermo, 48C | 3% for CO |
| S2 | MR13: MR13-04, 05, 06, 14-01, 02 | Thermo, 48C | 3% for CO |
| S3 | MR14: MR14-04, 05, 06 | Thermo, 48C | 3% for CO |
| S4 | MR15: MR15-03, 04, 05 | Thermo, 48C | 3% for CO |
| S5 | MR16: MR16-06, 08, 09 | Thermo, 48C | 3% for CO |
| S6 | MR17: MR17-05C, 08 | Thermo, 48C | 3% for CO |
| S7 | MR18: MR18-04, 05C, 06 | Thermo, 48C | 3% for CO |
| S8 | MR19: MR19-03C, 04 | Thermo, 48C | 3% for CO |
| S9 | MR20: MR20-E01, 05C, E02, 01 | Thermo, 48iTLE | 3% for CO |
| S10 | MR21: MR21-01, 03, 05C, 06 | Thermo, 48iTLE | 3% for CO |
| S11 | KH-18-6 | Thermo, 48iTLE | 3% for CO |
| S12 | NAAMES1 | TSI 3010 | CO: ±(10 +5%) ppb |
| S13 | NAAMES2 | TSI 3010 | |
| S14 | NAAMES3 | TSI 3010 | |
| S15 | NAAMES4 | TSI 3010 | |
| S16 | ATOMIC | TSI 3010 | |
| S17 | DYNAMO | TSI 3010 | |
| S18 | WACS | TSI 3010 | |
| S19 | VOCALS | TSI 3010 | ± 2% n/cm3 |
| S20 | MAGE92 | N/A | |
| S21 | RITS93 | TSI 3076 | |
| S22 | RITS94 | TSI 3076 | |
| S24 | ACEASIA | TSI 3760 | |
| S25 | NEAQS 2002 | NO by $NO_2$ chemiluminescence (custom instrument) Conversion of | NO ±(4%+0.006 ppb); NO2 ±(7%+0.024 ppb) |

| | | | |
|---|---|---|---|
| | | NO2 to NO by broadband UV light from 500W Xe lamp | |
| S26 | NEAQS 2004 | CO AeroLaser AL-5002;NO Chemiluminescence instrument; $NO_2$ Photolysis of $NO_2$ and NO detection | CO ±(3% + 1 ppbv); NO ±(4.4%); NO2 The total estimated accuracy for NO2 when $NO_2/NO = 3$ is ±(6.5% + 93 pptv), increasing to ±11% when $NO_2/NO = 1$ and ±23% when $NO_2/NO = 0.33$. |
| S27 | TEXAQS 2006 | CO AL 5002, NO by ozone-induced Chemiluminescence, NO2 by photolysis, followed by ozone-induced chemiluminescence | CO: ±3%, NO 3.8% + 0.010 ppbv, see NO2_ppbv_var |
| S28 | ICEALOT | CO AL5002, NO is measured directly by ozone-induced chemiluminescence. $NO_2$ is partially photoyzed and measured as the difference in signal between a photoyzed and unphotolyzed sample., CNC | CO ± 4.1%, see NO_ppbv_unc and NO2_ppbv_unc |
| S29 | CalNex 2010 | CO N/A, NO, $NO_2$: N/A | CO N/A, NO, $NO_2$ N/A |
| S60 | MOSAiC | CO: Cavity ring-down spectrometer (Picarro model G2401) | manufacturer-specified precisions of 1.0 ppb for 20-s averages, CO 1.5 ppb (5 min) |
| S62 | AEROSOLS99-INDOEX | TSI 3010 | N/A |

15

**Table S2.** Methods and uncertainties of CO, NOx, and CN observations associated with $O_3$ observations from aircraft campaigns. See Table S7 for a list of acronyms.

| Label | Campaign | CO, NOx instrumentation | Uncertainty |
|---|---|---|---|
| A5 | PEM-West A | TDL, Chemiluminescence, PF/LIF | CO 1%, NO ±18%. $NO_2$ ±20% |
| A6 | PEM-West B | TDL, LIF | CO 1%, NO ±18% |
| A8 | PEM-Tropics A | TDL, TP-LIF, PF/TP-LIF | CO 1%, NO 63 ppt, $NO_2$ 12 ppt |
| A9 | PEM-Tropics B P3B | differential absorption IR, chemiluminescence | CO ±2%, NO, $NO_2$: 1.5 ppt |
| A10 | PEM-Tropics B DC8 | TDL, TP-LIF, PF/TP-LIF | CO ±2%, NO, $NO_2$: see original data files |
| A11 | TRACE-P P3B | TDLAS, chemiluminescence | ±2% (CO), ±8%(NO), ±20% ($NO_2$) |
| A12 | TRACE-P DC8 | TDLAS, TP-LIF | ±2% (CO), ±20-30% (NO, $NO_2$) |
| A13 | INTEX-NA | TDLAS, LIF | CO (5% or 1 ppb), NO, $NO_2$ (5 ppt, 10%) |
| A14 | INTEX-B DC8 | DACOM, LIF | CO: 5% or 1 ppb, NO, $NO_2$ 5%, 15% |
| A15 | INTEX-B C-130 | VUV-fluorescence, chemiluminescence | CO: ± 10%, ±(15+7% of the mixing ratio) pptv for NO, ±(15+10% of the mixing ratio) pptv for $NO_2$ |
| A16 | ARCTAS | TDLAS, chemiluminescence | CO: 2% or 2 ppb, NO: 7%, $NO_2$: 10% |
| A17 | SEAC4RS DC8 | CO: Diode laser spectrometer, NO: chemiluminescence, $NO_2$:UV-LED photolysis/chemiluminescence | CO: 5% or 5 ppb, NO:0.010 ppbv + 4%, $NO_2$: 0.030 ppbv + 7% |
| A18 | SEAC4RS ER2 | CO: Picarro Cavity Ringdown Spectrometer | CO: 2.5 ppb |
| A19 | DISCOVER-AQ | 4ch chemiluminescence | 10 pptv + 10% for NO, 20 pptv + 10% for $NO_2$ |
| A20 | KORUS-AQ | 4ch chemiluminescence, CO: Diode laser spectrometer | (30 pptv + 20%) for NO, (50 pptv + 30%) for $NO_2$, 2% or 2 ppbv for CO |

| | | | |
|---|---|---|---|
| A21 | ATom1-4 | 4ch chemiluminescence, PICARRO cavity ringdown spectrometer | NO, $NO_2$: 5-10 ppt, 3.6 ppb CO (10 s) |
| A22 | HIPPO | VUV fluorescence | CO: 5 ppb |
| A23 | ACSIS FAAM | CO: AERO AL5002 instrument | N/A |
| A24 | ACCACIA FAAM | CO: AERO AL5002 instrument | N/A |
| A25 | CAST FAAM | CO: AERO AL5002 instrument | N/A |
| A26 | CLARIFY FAAM | CO: AERO AL5002 instrument | N/A |
| A27 | ITOP FAAM | CO: AERO AL5002 instrument | N/A |
| A28 | VOCALS FAAM | CO: AERO AL5002 instrument | N/A |
| A31 | TEXAQS2000 | CO vacuum ultraviolet fluorescence; $NO/O_3$ Chemiluminescence; $NO_2$ via UV photolysis | CO random uncertainty: 2.5%. NO: ±(20 pptv+5%); $NO_2$: ±(40 pptv+8%); |
| A32 | ITCT2002 | CO vacuum ultraviolet fluorescence; $NO/O_3$ Chemiluminescence; $NO_2$ via UV photolysis | CO random uncertainty: 2.5%. NO: ±(10 pptv+5%); $NO_2$: ±(30 pptv+10%) |
| A33 | ITCT2004 | CO VUV resonance fluorescence; NO, $NO_2$: Photolysis & $NO/O_3$ Chemiluminescence | CO 5%, NO_ppbv ±(0.010 + 5%); $NO_2$_ppbv ±(0.025 + 8%) |
| A35 | TEXAQS2006 | CO VUV resonance fluorescence; NO, $NO_2$: Photolysis & $NO/O_3$ Chemiluminescence | CO 5% ±1 ppbv, NO (0.015 ppbv + 5%), $NO_2$ (0.040 ppbv + 9%) |
| A36 | ARCPAC2008 | CO VUV Resonance Fluorescence, NO, $NO_2$: Photolysis and $NO/O_3$ Chemiluminescence | CO 3%, NO (0.02 + 8%), $NO_2$ (0.04 + 10%) |

| | | | |
|---|---|---|---|
| A37 | CalNex2010 | CO VUV Resonance Fluorescence, NO, $NO_2$: Photolysis and $NO/O_3$ Chemiluminescence | CO 5%, NO (0.01 ppbv + 3%), $NO_2$ (0.03 ppbv + 4%) |
| A45 | ACTIVATE | CO: Picarro Cavity Ringdown Spectrometer | CO ±5 ppb or ±2% |
| A46 | CONTRAST | 2-ch chemiluminescence instrument for NO-NO2, CO: Aero-laser AL5002 VUV fluorescence | CO: 3 ppbv ±3%, See error columns in this original file |
| A47 | TORERO | CO: Aero-laser AL5002 VUV fluorescence | CO: 3 ppbv ±3% |

**Table S3.** List of ozonesonde data contained in the ozonesonde data file. See Table S7 for a list of acronyms.

| Label | Station | Latitude | Longitude | Year begin | Year end | Data number | Wind directions for oceanic air masses (see footnote) | Regions | Literature | Data source |
|---|---|---|---|---|---|---|---|---|---|---|
| O1 | Alert | 82.50 | -62.33 | 2000 | 2020 | 23211 | all wind directions | R10 | | HEGIFTOM_homogenized |
| O2 | Eureka | 79.99 | -85.94 | 2000 | 2021 | 33473 | all wind directions | R10 | | HEGIFTOM_homogenized |
| O3 | Resolute | 74.71 | -94.97 | 2000 | 2021 | 19146 | all wind directions | R10 | | HEGIFTOM_homogenized |
| O4 | Scoresbysund | 70.48 | -21.95 | 1989 | 2022 | 38362 | all wind directions | R10 | | HEGIFTOM_homogenized |
| O5 | Sodankyla | 67.36 | 26.62 | 1994 | 2022 | 35893 | all wind directions | R10 | | HEGIFTOM_homogenized |
| O6 | Trinidad Head | 41.06 | -124.15 | 1997 | 2021 | 31441 | 5, 6 or 7 | R1 | | HEGIFTOM_homogenized |
| O7 | Wallops Island | 37.90 | -75.70 | 1995 | 2020 | 36700 | 2, 3 or 4 | R7 | Witte et al., (2019) | HEGIFTOM_homogenized |
| O8 | Izana | 28.46 | -16.26 | 1995 | 2022 | 35025 | all wind directions | R7 | | HEGIFTOM_homogenized |
| O9 | Hanoi | 21.02 | 105.80 | 2004 | 2018 | 6537 | | R2 | | HEGIFTOM_homogenized |
| O10 | Hilo | 19.72 | -155.05 | 1982 | 2021 | 39389 | all wind directions | R2 | | HEGIFTOM_homogenized |
| O11 | Costa Rica | 9.98 | -84.21 | 2005 | 2020 | 10920 | | R8 | | HEGIFTOM_homogenized |
| O12 | Paramaribo | 5.81 | -55.21 | 1999 | 2021 | 20597 | 0, 1, 2, 5, 6 or 7 | R8 | | HEGIFTOM_homogenized |
| O13 | Kuala Lumpur | 2.73 | 101.70 | 1998 | 2019 | 10985 | | R2 | | HEGIFTOM_homogenized |
| O14 | San Cristobal | -0.92 | -89.60 | 1998 | 2016 | 10405 | all wind directions | R2 | | HEGIFTOM_homogenized |
| O15 | Natal | -5.40 | -35.40 | 1998 | 2019 | 17505 | all wind directions | R8 | | HEGIFTOM_homogenized |
| O16 | Watukosek | -7.60 | 112.70 | 1998 | 2013 | 8404 | | R2 | | HEGIFTOM_homogenized |
| O17 | Ascension Island | -7.56 | -14.22 | 1998 | 2020 | 18238 | all wind directions | R8 | | HEGIFTOM_homogenized |
| O18 | Samoa | -14.33 | -170.71 | 1986 | 2021 | 25066 | all wind directions | R2 | | HEGIFTOM_homogenized |

| | | | | | | | | | | |
|---|---|---|---|---|---|---|---|---|---|---|
| O19 | Suva_Fiji | -18.15 | 178.45 | 1997 | 2021 | 11779 | all wind directions | R2 | | HEGIFTOM_ homogenized |
| O20 | Reunion | -21.10 | 55.50 | 1998 | 2020 | 18470 | all wind directions | R5 | | HEGIFTOM_ homogenized |
| O21 | McMurdo | -78.85 | 166.67 | 1986 | 2010 | 20440 | all wind directions | R11 | | HEGIFTOM_ homogenized |
| O22 | South Pole | -90.00 | -169.00 | 1967 | 2021 | 24122 | all wind directions | R11 | | HEGIFTOM_ homogenized |
| O23 | Isabela-San Cristobal | -0.96, -0.92 | -90.97, -89.6 | 2011 | 2011 | 400 | all wind directions | R2 | Gómez Martín et al. (2016) | Campaign (ECC) |
| O24 | Lauder | -45.04 | 169.68 | 1986 | 2021 | 44796 | | R3 | | HEGIFTOM_ homogenized |
| O25 | Ny Ålesund | 78.93 | 11.95 | 1992 | 2022 | 63633 | all wind directions | R10 | | HEGIFTOM_ homogenized |
| O26 | Shoyomaru | variable, see data | variable, see data | 1999 | 1999 | 350 | all wind directions | R2 | Shiotani et al. (2002), Fujiwara et al. (2003) | Campaign (ECC) |
| O27 | Marambio | -64.23 | -56.62 | 1988 | 2019 | 28057 | all wind directions | R11 | | WOUDC (ECC) |
| O28 | Davis | -68.58 | 77.97 | 2006 | 2023 | 16201 | all wind directions | R11 | | WOUDC (ECC) |
| O29 | Syowa | -69.01 | 39.58 | 2010 | 2023 | 16925 | all wind directions | R11 | | WOUDC (ECC only) |

Note: wind direction codes are [0=N, 1=NE, 2=E, …, and 7=NW]. Recommendations for Trinidad Head, Wallops Island, and Paramaribo was provisionally included.

**Table S4.** List of non-polar ground-based observations contained in the coastal sites dataset.

| Label | Station | Latitude | Longitude | Altitude (m) | Year begin | Year end | Data number | Ancillary data | Data source | Region | Literature |
|---|---|---|---|---|---|---|---|---|---|---|---|
| C1 | American Samoa | -14.25 | -170.56 | 77 | 1975 | 2015 | 296716 | N/A | TOAR-II DB | R2 | |
| C2 | Trinidad Head | 41.05 | -124.15 | 107 | 2002 | 2021 | 144515 | N/A | TOAR-II DB | R1 | |
| C3 | Tudor Hills | 32.27 | -64.88 | 30 | 1988 | 2021 | 205951 | N/A | TOAR-II DB | R7 | |
| C4 | Ragged Point | 13.17 | -59.43 | 45 | 1989 | 2017 | 121400 | N/A | TOAR-II DB | R8 | |
| C5 | Minamitorishima | 24.29 | 153.98 | 7 | 1994 | 2020 | 227252 | N/A | TOAR-II DB | R1 | |
| C6 | Cape Hedo | 26.87 | 128.25 | 68 | 2000 | 2021 | 182731 | N/A | EANET, https://monitoring.eanet.asia/document/signin/index | R1 | |
| C7 | Ogasawara | 27.09 | 142.22 | 212 | 2000 | 2021 | 175470 | N/A | EANET, https://monitoring.eanet.asia/document/signin/index | R1 | |
| C8 | Kennaook-Cape Grim | -40.68 | 144.69 | 94 | 1981 | 2020 | 301842 | N/A | CSIRO | R3 | Galbally et al. (2000) |
| C9 | Mace Head | 53.33 | -9.9 | 8 | 1988 | 2021 | 286705 | N/A | TOAR-II DB | R7 | |
| C10 | Cabo Verde | 16.86 | -24.87 | 10 | 2006 | 2022 | 134538 | CO | TOAR-II DB | R8 | |
| C11 | Cape Point | -34.35 | 18.49 | 230 | 2015 | 2021 | 40613 | N/A | TOAR-II DB | R9 | |
| C12 | Ushuaia | -54.85 | -68.31 | 18 | 1994 | 2022 | 202431 | N/A | TOAR-II DB | R9 | |
| C13 | Baring Head | -41.41 | 174.87 | 85 | 1991 | 2021 | 211900 | N/A | TOAR-II DB | R3 | |
| C14 | Mauna Loa | 19.54 | -155.58 | 3397 | 1957 | 2021 | 412530 | N/A | TOAR-II DB | R2 | |
| C15 | Sable Island | 43.93 | -59.9 | 8 | 2003 | 2014 | 78813 | NO, $NO_2$, NOx | TOAR-II DB | R7 | |
| C16 | Izana | 28.31 | -16.5 | 2373 | 1987 | 2022 | 300331 | N/A | TOAR-II DB | R7 | |
| C17 | Faial | 38.61 | -28.63 | 310 | 2007 | 2020 | 98546 | NO, $NO_2$, NOx | TOAR-II DB | R7 | |
| C18 | Cheeka Peak | 48.3 | -124.62 | 466 | 2006 | 2022 | 113646 | CO | TOAR-II DB | R1 | |
| C19 | Bukit Kototabang | -0.2 | 100.32 | 864 | 2007 | 2021 | 93431 | N/A | TOAR-II DB | R2 | |
| C20 | SanCristobal_Galapagos | -0.9 | -89.61 | 14 | 2000 | 2012 | 16477 | N/A | campaign | R2 | Gómez Martín et al. (2016) |
| C21 | Isabela_Island | -0.96 | -90.97 | 5 | 2010 | 2011 | 4419 | $NO_2$ | campaign | R2 | Gómez Martín et al. (2016) |

**Table S5.** List of polar ground-based observations contained in the polar sites dataset.

| Label | Station | Latitude | Longitude | Altitude (m) | Year begin | Year end | Data number | Ancillary data | Data source | Region |
|---|---|---|---|---|---|---|---|---|---|---|
| P1 | Barrow | 71.32 | -156.61 | 11 | 1973 | 2021 | 399426 | N/A | TOAR-II DB | R10 |
| P2 | South Pole | -90.0 | -24.8 | 2841 | 1975 | 2021 | 383899 | N/A | TOAR-II DB | R11 |
| P3 | Syowa | -69.01 | 39.59 | 16 | 1997 | 2022 | 208564 | N/A | TOAR-II DB | R11 |
| P4 | Alert | 82.45 | -62.51 | 210 | 1992 | 2022 | 228231 | N/A | Canadian data site https://data-donnees.az.ec.gc.ca/data/air/monitor/national-air-pollution-surveillance-naps-program/Data-Donnees/?lang=en | R10 |
| P5 | Arrival Heights | -77.83 | 166.66 | 184 | 1996 | 2021 | 204240 | N/A | TOAR-II DB | R11 |
| P6 | Villum | 81.6 | -16.67 | 20 | 2001 | 2021 | 106839 | N/A | TOAR-II DB | R10 |
| P7 | Pallas | 67.97 | 24.12 | 565 | 1995 | 2020 | 216419 | $NO_2$ | TOAR-II DB | R10 |
| P8 | Neumayer | -70.67 | -8.27 | 42 | 1995 | 2021 | 203827 | N/A | TOAR-II DB | R11 |
| P9 | Zeppelin mountain | 78.91 | 11.89 | 474 | 1989 | 2022 | 219504 | CO | TOAR-II DB | R10 |
| P10 | Karasjok | 69.47 | 25.22 | 333 | 1997 | 2010 | 109445 | N/A | TOAR-II DB | R10 |
| P11 | Concordia | -75.1 | 23.33 | 3233 | 2006 | 2022 | 91958 | N/A | TOAR-II DB | R11 |
| P12 | Halley | -75.62 | -26.18 | 30 | 2007 | 2022 | 88916 | N/A | TOAR-II DB | R11 |
| P13 | Esrange | 67.88 | 21.07 | 475 | 1990 | 2021 | 267012 | N/A | TOAR-II DB | R10 |
| P14 | Tiksi | 71.59 | 128.92 | 8 | 2010 | 2018 | 51107 | N/A | TOAR-II DB | R10 |
| P15 | Tustervatn | 65.83 | 13.91 | 439 | 1989 | 2022 | 275764 | N/A | TOAR-II DB | R10 |
| P16 | Summit | 72.58 | -38.48 | 3238 | 2000 | 2021 | 169281 | N/A | TOAR-II DB | R10 |
| P17 | Belgrano | -77.87 | -34.62 | 256 | 2007 | 2023 | 138284 | N/A | INTA | R11 |

**Table S6.** Statistics on the number of observation days per region and season.

| | Ship/buoy | | | | Airborne | | | | Ozonesonde | | | |
|---|---|---|---|---|---|---|---|---|---|---|---|---|
| | **DJF** | **MAM** | **JJA** | **SON** | **DJF** | **MAM** | **JJA** | **SON** | **DJF** | **MAM** | **JJA** | **SON** |
| **R1** | 97 | 293 | 241 | 218 | 159 | 204 | 49 | 26 | 262 | 372 | 370 | 270 |
| **R2** | 231 | 116 | 102 | 97 | 57 | 65 | 9 | 51 | 1149 | 1187 | 1251 | 1257 |
| **R3** | 131 | 159 | 24 | 140 | 12 | 15 | 13 | 21 | 455 | 462 | 464 | 583 |
| **R4** | 76 | 27 | 17 | 109 | 0 | 0 | 0 | 0 | 0 | 0 | 0 | 0 |
| **R5** | 179 | 73 | 24 | 41 | 0 | 0 | 0 | 1 | 182 | 206 | 160 | 200 |
| **R6** | 0 | 0 | 0 | 0 | 0 | 0 | 0 | 0 | 0 | 0 | 0 | 0 |
| **R7** | 220 | 521 | 415 | 350 | 19 | 52 | 93 | 77 | 695 | 690 | 773 | 678 |
| **R8** | 348 | 334 | 133 | 284 | 10 | 5 | 16 | 24 | 685 | 718 | 762 | 733 |
| **R9** | 319 | 228 | 98 | 214 | 0 | 0 | 0 | 2 | 0 | 0 | 0 | 0 |
| **R10** | 560 | 962 | 1156 | 1292 | 3 | 44 | 44 | 2 | 2840 | 2418 | 1596 | 1668 |
| **R11** | 567 | 166 | 108 | 113 | 1 | 1 | 0 | 2 | 925 | 784 | 1349 | 2427 |

**Table S7.** List of acronyms and abbreviations.

| Acronym | Definition |
|---|---|
| ACCACIA | Aerosol-Cloud Coupling and Climate Interactions in the Arctic |
| ACE-Asia | Aerosol Characterization Experiment – Asia |
| ACSIS | Atmospheric Chemistry and Climate of the Southern Indian Ocean |
| ACTIVATE | Aerosol Cloud meTeorology Interactions oVer the western ATlantic Experiment |
| AEROSOLS99-INDOEX | Indian Ocean Experiment 1999 |
| ARCPAC | Aerosol, Radiation, and Cloud Processes affecting Arctic Climate |
| ARCTAS | Arctic Research of the Composition of the Troposphere from Aircraft and Satellites |
| ATom | Atmospheric Tomography Mission |
| ATOMIC | Atlantic Tradewind Ocean–Atmosphere Mesoscale Interaction Campaign |
| CalNex | California Nexus |
| CAST | Coordinated Airborne Studies in the Tropics |
| CLARIFY | Cloud-Aerosol-Radiation Interactions and Forcing: Year 2017 |
| CONTRAST | Convective Transport of Active Species in the Tropics |
| DISCOVER-AQ | Deriving Information on Surface Conditions from Column and Vertically Resolved Observations Relevant to Air Quality |
| DYNAMO | Dynamics of the Madden-Julian Oscillation |
| ECC | Electrochemical concentration cell |
| HEGIFTOM | Harmonization and Evaluation of Ground-based Instruments for Free-Tropospheric Ozone Measurements |
| HIPPO | HIAPER Pole-to-Pole Observations |
| ICEALOT | International Chemistry Experiment in the Arctic LOwer Troposphere |
| INTEX-B | Intercontinental Chemical Transport Experiment-B |
| INTEX-NA | Intercontinental Chemical Transport Experiment-North America |
| ITCT | Intercontinental Transport and Chemical Transformation |
| ITOP | Intercontinental Transport of Ozone and Precursors |
| KORUS-AQ | Korea-United States Air Quality Study |
| MAGE | Marine Aerosol and Gas Exchange |
| MOSAiC | Multidisciplinary drifting Observatory for the Study of Arctic Climate |
| NAAMES | North Atlantic Aerosols and Marine Ecosystems Study |
| NEAQS | New England Air Quality Study |
| PEM-Tropics | Pacific Exploratory Mission-Tropics |
| PEM-West | Pacific Exploratory Mission-West |
| RITS | Research in the Tropics |
| SEAC4RS | Studies of Emissions and Atmospheric Composition, Clouds and Climate Coupling by Regional Surveys |
| TEXAQS | Texas Air Quality Study |
| TORERO | Tropical Ocean tRoposphere Exchange of Reactive halogen species and Oxygenated VOC |
| TRACE-P | Transport and Chemical Evolution over the Pacific |
| VOCALS | VAMOS Ocean-Cloud-Atmosphere-Land Study |
| WACS | Western Atlantic Climate Study |

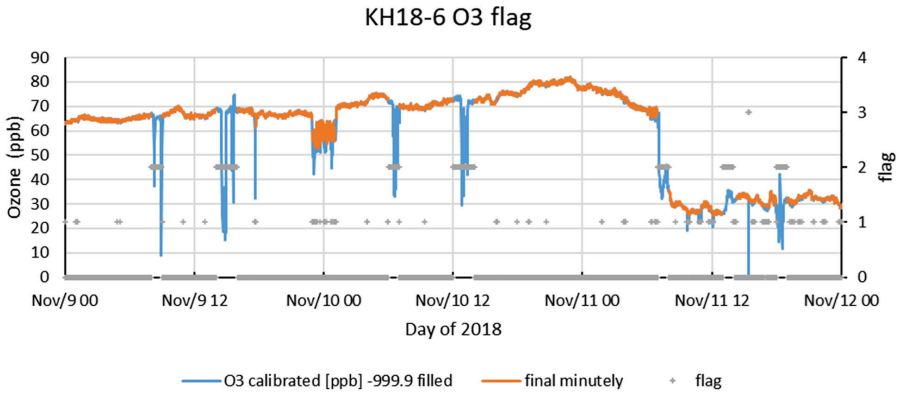


**Figure S1.** Removal of ozone data affected by ship exhaust and instability (blue). Flags (grey, in the right axis) 1: 1-minute based data removed (as lower than hourly average - 1σ), 2: hours with large variability, and 3: no data. The data after removal (orange) are used to calculate the hourly averages.

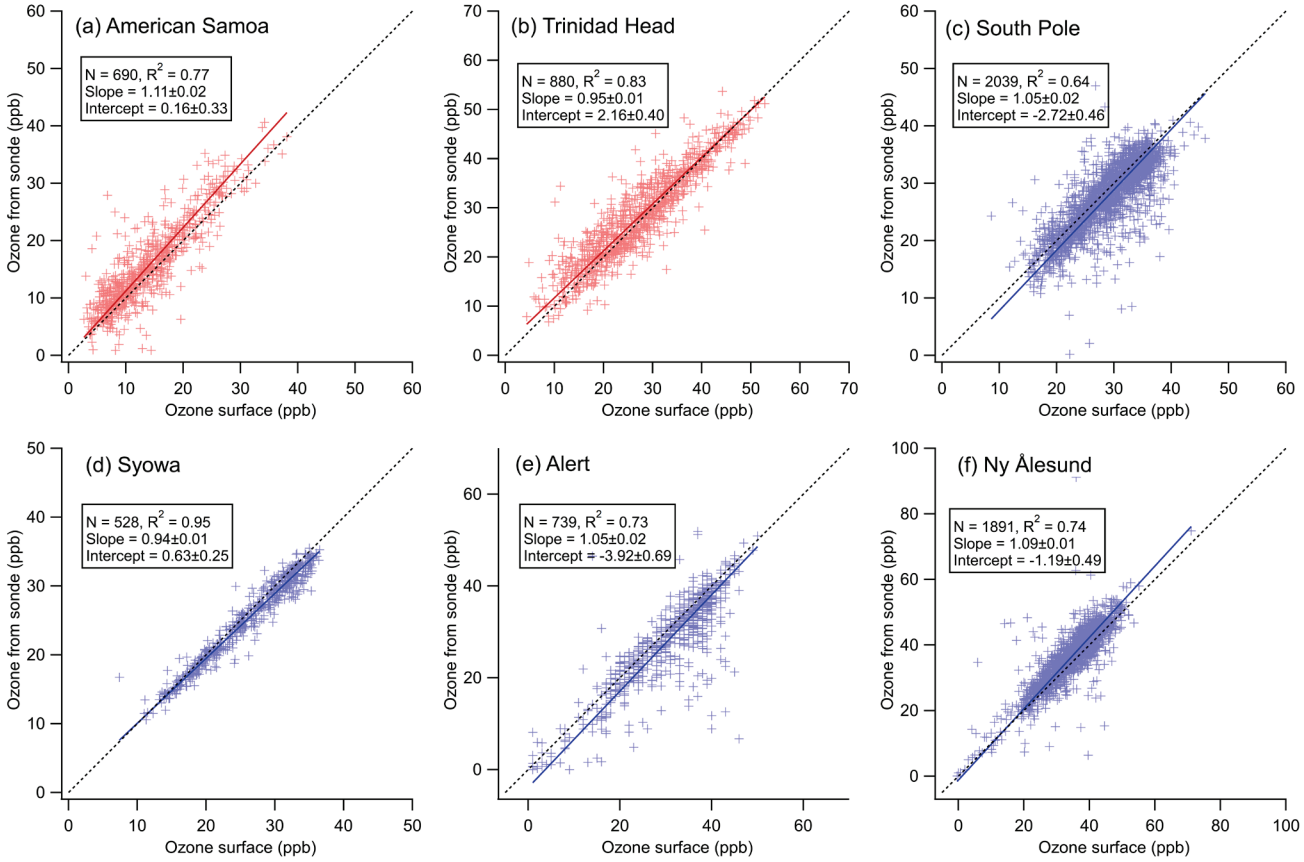


**Figure S2.** Scatterplots between ozonesonde data at the lowest level (~200 m) and surface data at 6 sites with co-located observations. Two sites (red) are from non-polar regions and the other four sites (blue) are from polar regions. The colored lines are the bivariate linear fits. The dashed black lines represent y = x.

**References**

Fujiwara, M., Xie, S.-P., Shiotani, M., Hashizume, H., Hasebe, F., Vömel, H., Oltmans, S. J., and Watanabe, T.: Upper-tropospheric inversion and easterly jet in the tropics, J. Geophys. Res., 108 (D24), 2796, https://doi.org/10.1029/2003JD003928, 2003.

Galbally, I. E., Bentley, S. T., and Meyer, C. P.: Mid-latitude marine boundary layer ozone destruction at visible sunrise observed at Cape Grim, Tasmania, 41° S, Geophys. Res. Lett., 27, 3841–3844, https://doi.org/10.1029/1999GL010943, 2000.

Gómez Martín, J. C., H. Vömel, T. D. Hay, A. S. Mahajan, C. Ordóñez, M. C. Parrondo Sempere, M. Gil-Ojeda, and A. Saiz-Lopez, On the variability of ozone in the equatorial eastern Pacific boundary layer, J. Geophys. Res. Atmos., 121, 11,086–11,103, https://doi.org/10.1002/2016JD025392, 2016.

Shiotani, M., Fujiwara, M., Hasebe, F., Hashizume, H., Vömel, H., Oltmans, S. J., and Watanabe, T.: Ozonesonde observations in the equatorial Eastern Pacific - the Shoyo-maru survey -, J. Meteorol. Soc. Jpn., 80, No. 4B, 897-909, https://doi.org/10.2151/jmsj.80.897, 2002.

Witte, J. C., Thompson, A. M., Schmidlin, F. J., Northam, E. T., Wolff, K. R., and Brothers, G. B.: The NASA Wallops Flight Facility digital ozonesonde record: Reprocessing, uncertainties, and dual launches. J. Geophys. Res. Atmos., 124, 3565–3582. https://doi.org/10.1029/2018JD030098, 2019.